Lab on a Chip

Microfluidic-based capture and release of cancer-derived exosomes via peptide-nanowire hybrid interface

Journal:	*Lab on a Chip*
Manuscript ID	LC-ART-09-2020-000899.R1
Article Type:	Paper
Date Submitted by the Author:	25-Nov-2020

Complete List of Authors:	Suwatthanarak, Thanawat; Tokyo Institute of Technology School of Materials and Chemical Technology, Chemical Science and Engineering Thiodorus, Ivan; Nagoya University Tanaka, Masayoshi; Tokyo Institute of Technology, Department of Chemical Engineering Shimada, Taisuke; Nagoya University, Department of Biomolecular Engineering Takeshita, Daiki; Nagoya University, Department of Biomolecular Engineering Yasui, Takao; Nagoya University, Department of Applied Chemistry Baba, Yoshinobu; Nagoya University, ImPACT Research Center for Advanced Nanobiodevices Okochi, Mina; Tokyo Institute of Technology,

ARTICLE

Microfluidic-based capture and release of cancer-derived exosomes via peptide-nanowire hybrid interface†

Received 00th January 20xx,
Accepted 00th January 20xx

DOI: 10.1039/x0xx00000x

Thanawat Suwatthanarak,[a] Ivan Adiyasa Thiodorus,[b] Masayoshi Tanaka,[a] Taisuke Shimada,[b] Daiki Takeshita,[b] Takao Yasui,[*bc] Yoshinobu Baba,[*bd] and Mina Okochi,[*a]

Cancer-derived circulating exosomes or nanoscale extracellular vesicles are emerging biomarkers for disease detection and treatment because of their cell-specific constituents and unique intercellular pathways. For efficient exosome isolation from bio-fluids, the design of high-affinity nanointerfaces is of great importance in the development of miniaturized systems for the collection of exosomes. Herein, we report peptide-functionalized nanowires as a biorecognition interface for the capture and release of cancer-derived exosomes within a microfluidic channel. Based on the amino-acid sequence of EWI-2 protein, a partial peptide that bound to CD9 exosome marker and thus targeted cancer exosomes was screened. Linkage of the exosome-targeting peptide with a ZnO-binding sequence allowed one-step and reagent-free peptide modification of the ZnO nanowire array. As a result of peptide functionalization, the exosome-capturing ability of ZnO nanowires was significantly improved. Furthermore, the captured exosomes could be subsequently released from the nanowires under a neutral salt condition for downstream applications. This engineered surface that enhances the nanowires' efficiency in selective and controllable collection of cancer-derived exosomes provides an alternative foundation for developing microfluidic platforms for exosome-based diagnostics and therapeutics.

Introduction

Exosomes represent a nano-sized subset of extracellular vesicles (typically 40–200 nm in diameter) secreted from most cell types into biological fluids, such as blood, urine, saliva, and cell-culture medium.[1,2] Exosomes carry many biomolecules (e.g., lipids, proteins, nucleic acids) similar to those of their parent cells, and are involved in intercellular transport and communication.[3,4] Cancer cells are believed to release large numbers of exosomes carrying cancer-specific messenger molecules, which not only play an important role in cancer progression/metastasis but are also valuable as cancer biomarkers for pathological studies.[5,6] In addition, cancer exosomes have been explored as therapeutic agents, including cell-created drug cartridges or gene delivery vesicles for site-specific targeting, due to their unique intracellular pathways and organ/cell-specific tropism.[7,8] Therefore, cancer exosomes in non-invasive liquid biopsies are promising biomarkers, possessing broad biomedical applications for early detection and effective treatment.

Nonetheless, utilization of exosomes is faced with multiple, time-consuming steps in conventional laboratory methods for isolating exosomes (e.g., ultracentrifugation, filtration, size-exclusion chromatography, immunoaffinity purification) and analyzing their contents (e.g., western blotting, enzyme-linked immunosorbent assay (ELISA), polymerase chain reaction, flow cytometry).[9–13] Hence, miniaturized systems or lab-on-a-chip platforms, exploiting micro/nanotechnology, have been extensively investigated for rapid, convenient and on-site exosome separation expediting exosome studies.[14–24] Based on biochemical and physical properties of exosomes, microfluidic channels have been coupled with a wide range of exosome-isolating strategies, including immunoaffinity,[15,16] membrane filtration,[17,18] acoustics,[19,20] and nanowire tapping.[21–24] Following microfluidic-based exosome collection, some platforms have been additionally integrated with *in situ* exosome analytical techniques, including protein profiling,[16] ELISA,[17,18] and colorimetric assay.[23] Since these miniaturized systems have great potential for biomedical applications, development of an exosome-collecting nanointerface is essential to further design the next generation of exosome-based diagnostic and therapeutic platforms.

Recently, inorganic nanowires have attracted increasing attention for their mechanical stability and high surface-to-volume ratio,[25] as well as the fact that they are often embedded in micro-channels for analyzing and characterizing intracellular components (e.g., proteins, nucleic acids),[26,27] cells,[28,29] as well as exosomes.[21–24] In particular, ZnO nanowire arrays that have

[a] *Department of Chemical Science and Engineering, Tokyo Institute of Technology, 2-12-1 O-okayama, Meguro-ku, Tokyo 152-8552, Japan. Email: okochi.m.aa@m.titech.ac.jp*
[b] *Department of Biomolecular Engineering, Graduate School of Engineering, Nagoya University, Furo-cho, Chikusa-ku, Nagoya 464-8603, Japan*
[c] *Japan Science and Technology Agency (JST), PRESTO, 4-1-8 Honcho, Kawaguchi, Saitama 332-0012, Japan*
[d] *Institute of Nano-Life-Systems, Institutes of Innovation for Future Society, Nagoya University, Furo-cho, Chikusa-ku, Nagoya 464-8603, Japan*

† Electronic Supplementary Information (ESI) available: [Experimental, Fig. S1–S8 and Table S1 (PDF)]. See DOI: 10.1039/x0xx00000x

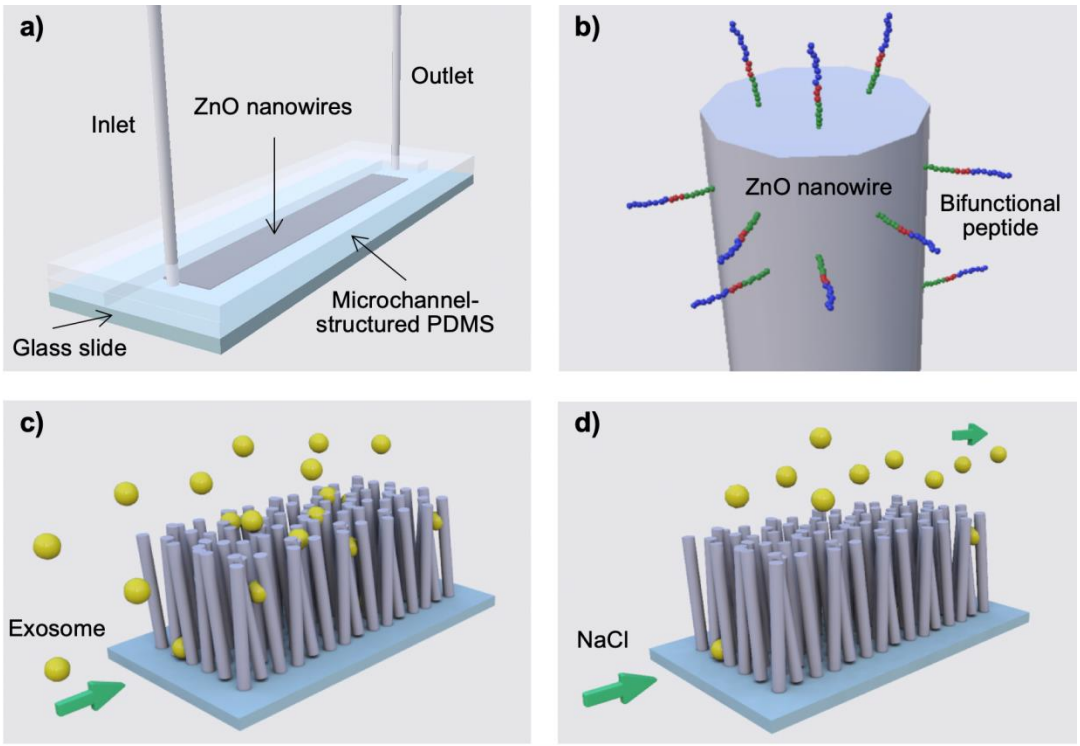

Fig. 1 Schematic illustrations of the peptide-nanowire interface within a microfluidic channel for capture and release of cancer-derived exosomes. (a) The platform configuration. PDMS, polydimethylsiloxane. (b) Modification of ZnO nanowire surface with a bifunctional peptide, consisting of a ZnO-binding site (green), a linker (red), and an exosome-binding site (blue). (c) Capture of exosomes by the peptide-modified nanowire interface. (d) Release of the captured exosomes from the nanowire interface using a NaCl solution.

good biocompatibility, negatively charged surfaces, and size-exclusion effects show promising results in microfluidic-based exosome entrapment from clinical urine[22] and serum[23] samples. Previously, nanowire-based devices provided rapid exosome capture, with some of them later allowing *in situ* exosome analyses, including miRNA extraction and colorimetric detection.[21–24] However, these unmodified and antibody-modified nanowires were dissolved to release the captured exosomes.[21,23,24] This may result in contamination of the collected exosomes by dissolution in an acidic solution and damage the nanowires, thus affecting their downstream applications.

In this study, we propose a peptide-nanowire interface that can effectively capture cancer-derived exosomes and release captured exosomes intact, without damage to the nanowires. A peptide binding to cancer exosomes was first screened from the amino-acid sequence of EWI-2 protein, a major partner of the CD9 exosome marker, using the peptide array technique. Subsequently, a ZnO nanowire array fabricated within a microfluidic prototype platform (Fig. 1a) was functionalized by incubation with a solution of the designed bifunctional peptide, consisting of a ZnO-binding site, a linker, and an exosome-binding site (Fig. 1b). Unlike the modification of antibodies against exosome-specific surface proteins (e.g., tetraspanin CD9, CD63, and CD81), the bifunctional peptide does not require any cross-linking in the immobilization step, providing a simple, bio-friendly, and ZnO surface-specific functionalization (Fig. 1b). By combining the ZnO nanowires' physicochemical properties and the peptide's biological interaction, the efficiency of nanowires in the capture and release of circulating cancer exosomes can be significantly enhanced (Fig. 1c and 1d). The bifunctional peptide allows the captured exosome to be released with neutral salt, a non-damaging condition to both nanowires and exosomes (Fig. 1d). The peptide-nanowire hybrid surface developed here will facilitate the development of exosome-based microfluidic systems, in which exosomes can be trapped and released, toward clinical analysis as well as medicinal utilization of intact exosomes as gene/drug carriers.

Results

Array-based screening of exosome-binding peptides

To screen for the functional peptides binding to cancer-derived exosomes, a library of eight-mer peptides derived from the human EWI-2 protein, a major partner of tetraspanin CD9 over-expressed in multiple cancer cells and exosomes, was constructed (Fig. S1).[30–32] CD9-positive exosomes, prepared from MDA-MB-231 human breast cancer cells and labeled with a fluorescent dye,[32,33] were utilized in a binding assay with an EWI-2 peptide array.[34–36] Fig. 2a shows a fluorescence image of the exosome-bound peptide array, used for spot intensity quantification (Fig. S2). Nine candidate peptides with spot intensities greater than two standard deviations from the mean of all spots are shown in Fig. 2b. Most candidates exhibited an isoelectric point above seven, hydrophilicity (negative grand average of hydropathy value), and a positive charge (Table S1). This suggested that polar and electrostatic properties play an

important role in the peptide-exosome interaction. Interestingly, a combined nest motif of R and L residues or an RLR motif was present in most candidate sequences (P238, P169, P237, P239, P182, P168, and P170) (Fig. 2b and Table S1). This RLR concavity is often found in functionally important regions and facilitates binding of anionic groups (e.g., phosphate or carboxylate groups) of enzymes and proteins, suggesting that these peptides were derived from the functional sites of EWI-2.[37,38] Moreover, all candidates were derived from the immunoglobulin 3 and 4 domains of EWI-2, which are necessary for interacting with the large extracellular loop of tetraspanins.[39,40] The preferential binding site of the highest binder P238 (RSHRLRLH) to CD9 was estimated using PepSite software.[41] Based on a protein/peptide structure database, the first-rank prediction revealed that P238 likely binds to the CD9 surface on the large extracellular loop near the outer membrane region (Fig. S3). These findings are consistent with a specific interaction between P238 and CD9 on the exosome surface.

The binding affinity between P238 and CD9 was further investigated using surface plasmon resonance (SPR). P238 was immobilized on the sensor chip's surface as a ligand before injection of CD9 protein. The SPR response gradually increased with increasing concentration of CD9 (Fig. 2c). The response was proportional to the mass of CD9 bound to the peptide-immobilized surface, implying an interaction between P238 and CD9. Using a steady-state model, a plot of stabilized SPR responses against CD9 concentrations revealed a dissociation constant (K_D) of 4.66×10^{-7} M. To assess P238's binding selectivity, CD9, EpCAM, or integrin beta 5 was flowed over the P238-immobilized chip. Fig. 2d shows that P238 preferentially bound to CD9 rather than to the other two well-known

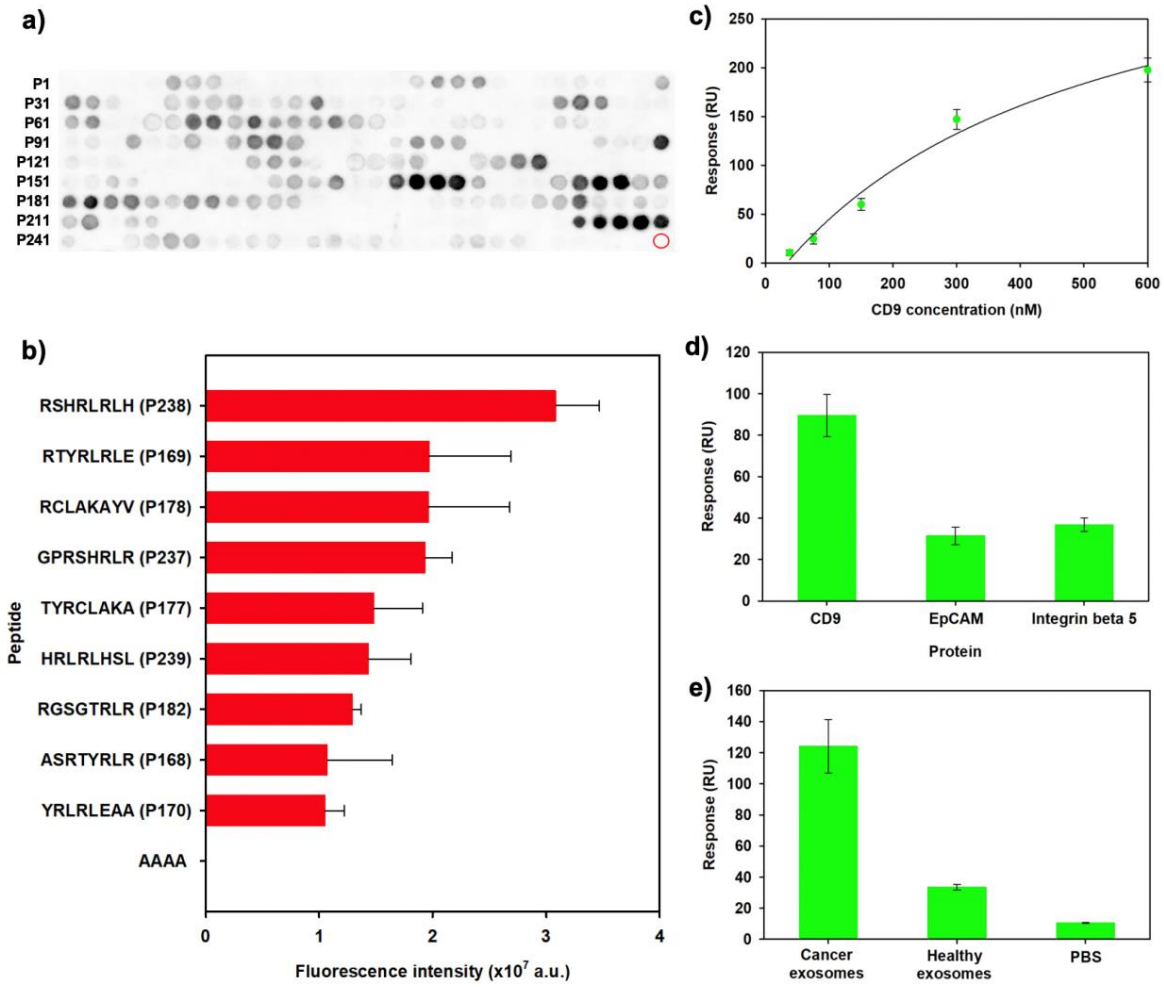

Fig. 2 Array-based screening of exosome-binding peptides from EWI-2 protein. (a) Representative fluorescence image of the EWI-2 peptide array after the binding assay with fluorescently labeled MDA-MB-231-derived cancer exosomes. The red circle denotes the AAAA peptide (a negative control). (b) Spot fluorescence intensities of the nine candidate peptides determined by ImageQuant software. (c) Stabilized SPR responses of P238-immobilized sensor chip against CD9 concentrations to determine the K_D for P238-CD9 binding. (d) SPR responses of P238-immobilized sensor chip to the flows of CD9, EpCAM, and integrin beta 5. (e) SPR responses of P238-immobilized sensor chip to the flows of cancer cell-derived exosomes, healthy human serum-derived exosomes, and phosphate-buffered saline (PBS). Error bars indicate the standard deviation (N=3).

exosome membrane proteins. Suspension of MDA-MB-231-derived cancer exosomes or healthy human serum-derived exosomes was also applied to compare the interaction with P238. Due to the higher expression of CD9 in cancer exosomes (688.0±45.6 pg/mL) than in healthy ones (150.2±6.6 pg/mL), a flow of cancer exosomes generated a higher SPR response than that of healthy ones (Fig. 2e). Although non-specific binding was observed (Fig. 2d), there was clear response difference between cancer and healthy exosomes, which was consistent with the CD9 expression level in both samples (Fig. 2e). Collectively, these results suggest that the P238 peptide mimics the function of its parent EWI-2 protein and has potential as a probe for tetraspanin CD9 as well as cancer-derived exosomes.

Enhanced exosome capture of microfluidic nanowire array by bifunctional peptide

To functionalize the ZnO surface with P238, a linear bifunctional peptide (HCVAHRGGGRSHRLRLH) consisting of a ZnO-binding site (HCVAHR),[42] a linker (GGG), and an exosome-binding site (P238; RSHRLRLH) was designed.[43,44] First, peptide bifunctionality was evaluated by incubating ZnO microparticles with a bifunctional peptide and then with cancer cell-derived exosomes. Overlaying of fluorescence micrographs revealed that the surface of the ZnO microparticles was modified with fluorescein-5-isothiocyanate (FITC)-conjugated peptide and bound to CellMask-stained exosomes (Fig. S4a). In contrast, no exosome binding was observed with a control peptide (HCVAHRGGGAAAA) in the absence of an exosome-binding site (Fig. S4b). This result confirmed the bifunctionality of the designed peptide before it was applied to modify the ZnO nanowire surface.

As shown in Figs. 3a and S5, a microfluidic prototype channel (2 cm in length, 2 mm in width, and 20 µm in height) containing a ZnO nanowire array at the bottom surface was constructed. Fig. 3b and 3c show field emission scanning electron microscopy (FESEM) images of ZnO nanowires approximately 50 nm in diameter and 1 µm in height, hydrothermally grown on a ZnO layer-deposited glass substrate. Modification of the nanowire interface inside a microchannel was achieved by simply injecting and incubating the bifunctional peptide solution to the platfrom. Using high-performance liquid chromatography (HPLC) quantification of the remaining peptide in solution, the amount of modified peptide was estimated to be 1.15±0.06 nmol/mm^2. FESEM observation of the modified nanowires also revealed that the diameter of the nanowires was slightly increased (Fig. S6a, b). Furthermore, p-polarized multiple-angle incidence resolution spectrometry (pMAIRS) was employed to analyze the molecular orientation of the peptide on nanowires. The bifunctional peptide-modified nanowires produced two main peaks derived from C=O and N-H groups in both the out-of-plane and in-plane pMAIRS spectra (Fig. 3d, left), implying that the peptide modification was accomplished in both the parallel and perpendicular directions of the nanowires.

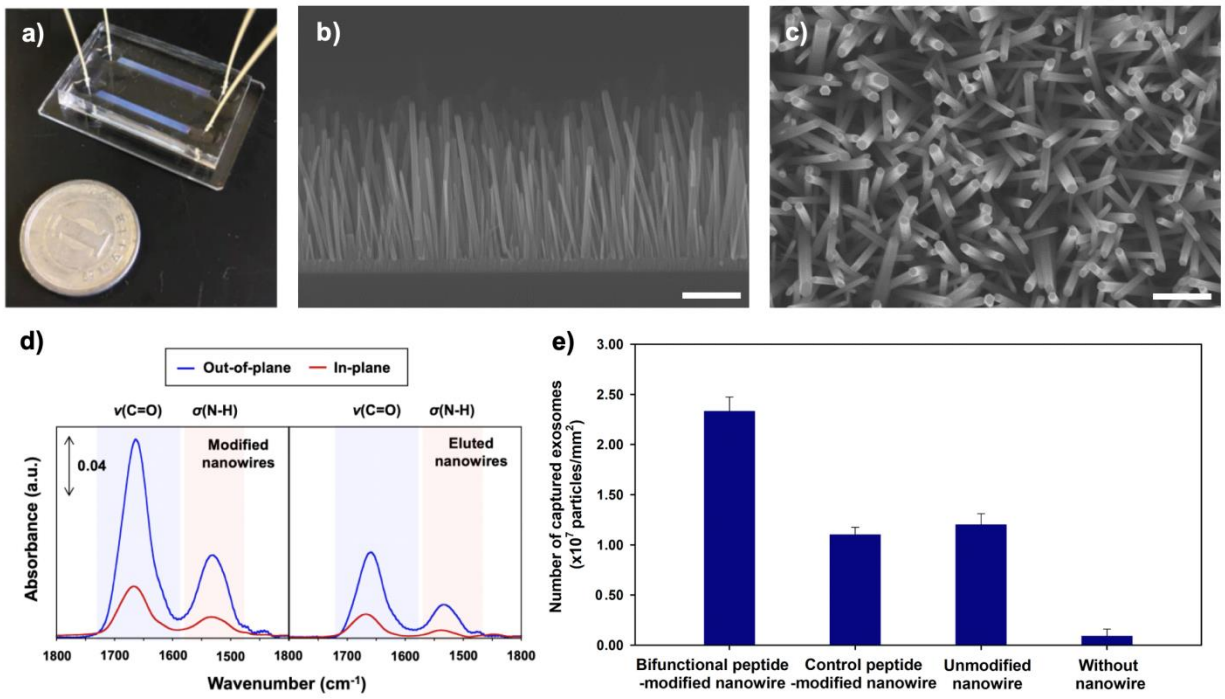

Fig. 3 Enhanced exosome capture of microfluidic nanowire array by bifunctional peptide. (a) An image of the double-channel platform relative to a one-Japanese yen coin (1.5 cm in diameter). One channel was used for one experiment. (b and c) FESEM images of the ZnO nanowires, hydrothermally grown on a glass substrate. Scale bar, 500 nm. (d) pMAIRS spectra of the peptide-modified nanowires before (left) and after (right) the peptide elution with 1 M NaCl solution. (e) NTA-based exosome capture ability. Error bars represent the standard deviation (N=3).

Conditions for peptide elution were then investigated by varying the concentration of NaCl salt, a common ion source for the peptide denaturation.[45] The fluorescence intensity of the FITC-conjugated bifunctional peptide modified on the nanowire surface decreased with increasing NaCl concentration, suggesting peptide elution (Fig. S6c). Based on these data, 1 M NaCl was chosen for eluting the peptide from the nanowires. After NaCl treatment, the nanowires maintained their structure (Fig. S6d), and elution of the peptide was confirmed by the large drop in two main C=O and N-H peaks of the pMAIRS spectra (Fig. 3d, right). These results clearly indicate that the bifunctional peptide enables a simple, non-covalent modification of the nanowire interface within a microfluidic channel and the modified peptide can be then eluted under a neutral condition.

To assess the exosome capture ability of the modified nanowires, a suspension of cancer cell-derived exosomes (1×10^9 particles/mL or 3.33×10^9 particles/mm^2) was introduced to the platform through an inlet tube, and a sample of uncaptured exosomes was collected by an outlet tube. The number of exosomes captured by the nanowires was estimated from the number of uncaptured exosomes, determined by a nanoparticle tracking analysis (NTA) system. The bifunctional peptide-modified nanowires captured $2.33\pm0.15\times10^7$ particles/mm^2; in comparison, the control peptide-modified and unmodified nanowires could capture $1.10\pm0.08\times10^7$ and $1.20\pm0.11\times10^7$ particles/mm^2, respectively (Fig. 3e). The modification by the bifunctional peptide provided a nearly 2-fold increase in exosome capture relative to unmodified nanowires (Fig. 3e). In addition, a control platform without nanowires showed negligible capture (Fig. 3e). These results demonstrate that the bifunctional peptide can enhance exosome capture upon peptide-exosome affinity.

Enhanced exosome release of microfluidic nanowire array by bifunctional peptide

To collect the captured exosomes from the peptide-modified nanowire interface, the elution solution (1 M NaCl) was introduced and the number of released exosomes was determined. As shown in Fig. 4a, NTA-based analysis indicated a significant increase in the exosome recovery percentage from less than 10% in the unmodified nanowires to approximately 70% in the bifunctional peptide-modified nanowires. This implied that exosome release could be achieved via peptide modification. FESEM revealed the presence of exosomes with a diameter of ~100 nm on the bifunctional peptide-modified nanowires after exosome capture (Fig. 4b and 4c) but not after exosome release (Fig. 4d and 4e). This finding shows that peptide modification allows the captured exosomes to be released under a neutral salt condition without nanowire damage, suggesting that nanowires can be reused, also preventing contamination of the released exosomes by nanowire contaminants.

Next, the released exosomes were characterized to evaluate their integrity. The size distribution of particles in the eluted exosome suspension was 80-160 nm, similar to that of the introduced exosomes (Fig. 4f). The released exosomes were observed to have a round morphology (Fig. 4f, insert). Zeta potential analysis revealed that the released exosomes possessed a negatively charged surface, similar to those of original exosomes, supporting the presence of freely existing exosomes not bound to the positively charged peptide in the eluted suspension (Fig. 4g). To demonstrate the compatibility of the released exosomes for downstream analysis, they were subjected to extraction of microRNA (miRNA), used as cancer biomarkers.[46,47] Fig. 4a shows that the amounts of extracted miRNA were in accordance with the recovery percentage of exosomes, suggesting that the released exosomes were intact and suitable for following analyses without any side effects caused by NaCl or peptides. Therefore, the functionalization of bifunctional peptide enhances nanowire ability for not only capture but also release of exosomes without nanowire and exosome damage.

Comparison of exosome-collecting efficiency between peptide-nanowire platform and ultracentrifugation

An ultracentrifugation technique was also performed in parallel to compare the exosome isolation efficiency. Fig. 5 shows the relative exosome amount in the exosome suspensions obtained from the peptide-nanowire platform and ultracentrifugation. The number of collected exosomes by the peptide-nanowire platform was $(6.9 \pm 0.7) \times 10^8$ cells/ml while it was $(1.8 \pm 0.2) \times 10^8$ cells/ml with the ultracentrifugation. The nanowire platform modified with bifunctional peptide yielded an almost 4-fold increase in exosome collection over conventional ultracentrifugation (Fig. 5). This result shows that the peptide-nanowire platform enables collection of exosomes superior to the standard ultracentrifugation method in terms of efficiency.

Evaluation of exosome-collecting efficiency from a cultured, cell-suspended medium

To demonstrate the potential of our platform under more complicated condition, the exosome-collecting efficiency from cell suspension added to the medium after cell growth was evaluated. The cultured medium of MDA-MB-231 cells was collected, suspended with MDA-MB-231 cells, and used as the complicated sample. Three components in the prepared and eluted samples, including exosomes, proteins, and cells, were quantified to evaluate the collecting efficiency of the peptide-modified nanowire platform in comparison to the unmodified nanowire platform. Unlike the previous results, the exosomes were quantified using exosome ELISA (CD9 detection). As shown in Fig. 6, the peptide-modified platform was more selective for capturing and releasing exosomes compared to the unmodified platform, suggesting that the peptide-nanowire interface could separate the exosomes from the complicated condition. Interestingly, the exosome-collecting efficiency of the peptide-modified platform from cell culture medium was 67%, which is the same as that from exosome-suspended PBS (~70%), while the collection efficiency using the peptide-unmodified platform decreased to 8.9%. An approximate 7.5-fold increase in collection efficiency of exosomes was obtained in the peptide-

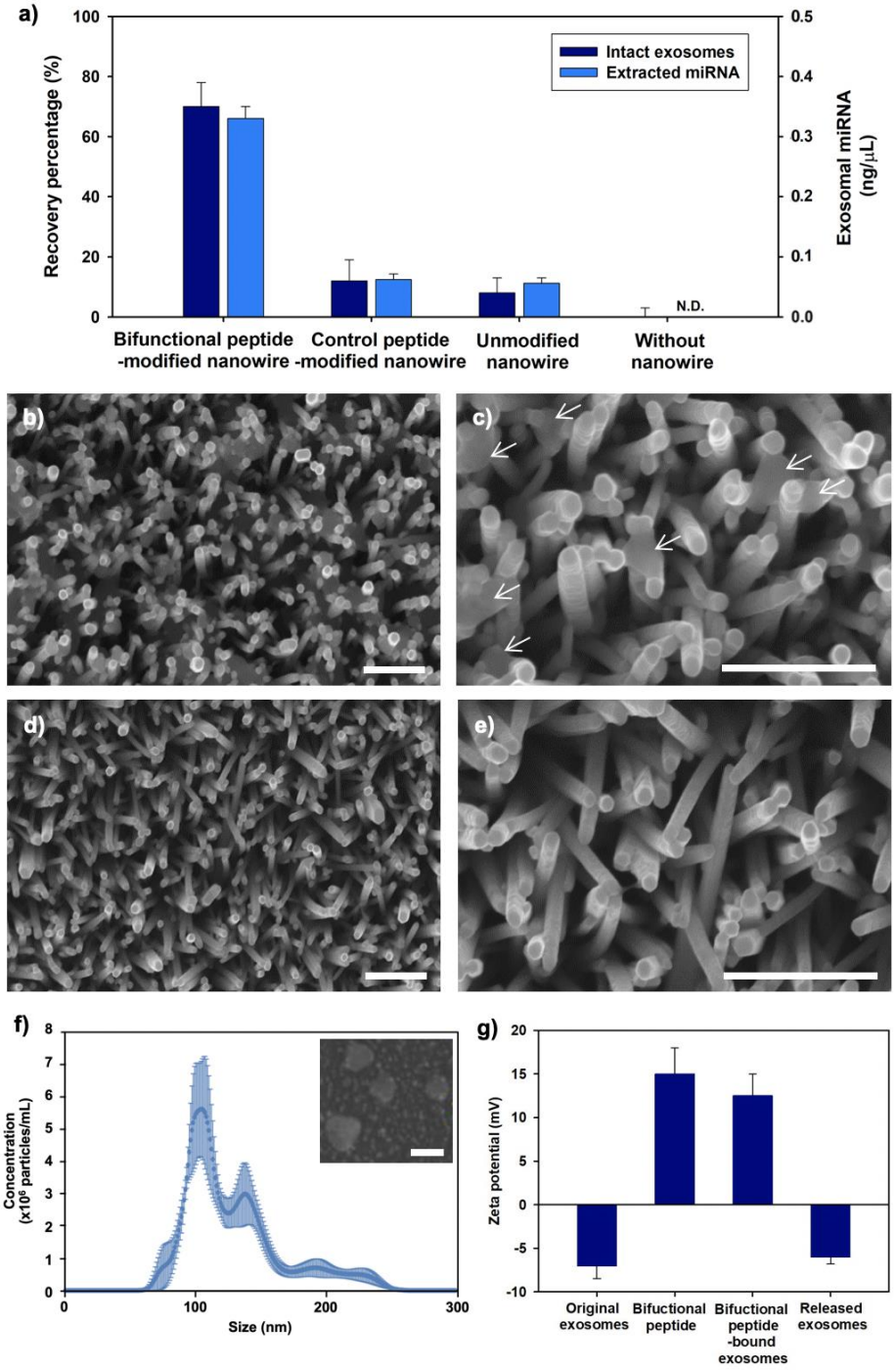

Fig. 4 Enhanced exosome release of microfluidic nanowire array by bifunctional peptide. (a) NTA-based exosome recovery percentage and quantification of exosomal miRNA in the released exosome suspensions. N.D., not detected. (b and c) FESEM images of the bifunctional peptide-modified ZnO nanowires after the exosome capture. Arrows indicate the exosome positions. (d and e) FESEM images of the nanowires after the exosome release. Scale bar, 500 nm. (f) NTA-based size distribution of the particles in the eluted exosome suspension from the bifunctional peptide-modified nanowire platform. Insert is a FESEM image of the eluted exosome sample dried on silicon wafer substrate with a 100 nm scale bar. (g) Zeta potential values of the original exosomes derived from MDA-MB-231 cells, the bifunctional peptide, the bifunctional peptide-bound exosomes, and the released exosomes from the bifunctional peptide-modified nanowire platform. Error bars denote the standard deviation (N=3).

modified nanowire platform compared to the unmodified nanowire platform. These data indicate that the peptide-nanowire interface was effective in the collection of exosomes in harsh conditions such as bio-fluid samples.

Discussion

In this study, we have explored an exosome-binding peptide via a protein-protein interaction and demonstrated its potential in nanowire-/microfluidic-based exosome collection with controllable capture and release features. We screened P238 peptide that mimic the function of EWI-2 for CD9 binding. Due to the affinity of P238 for CD9 and cancer exosomes, P238 holds promise for a broad range of exosome applications including diagnosis, imaging, targeting, and

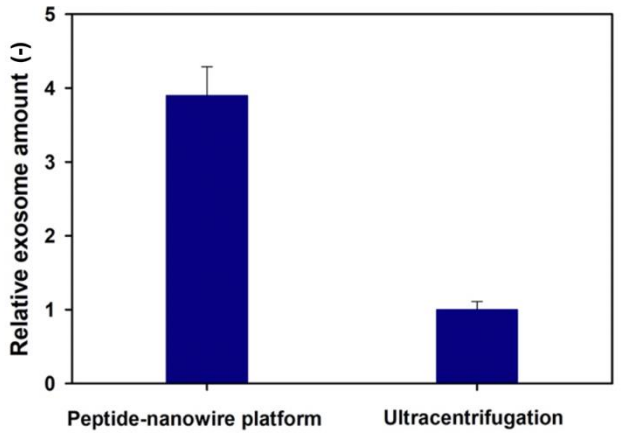

Fig. 5 Comparison of exosome isolation efficiency between peptide-nanowire platform and ultracentrifugation. Error bars represent the standard deviation (N=3).

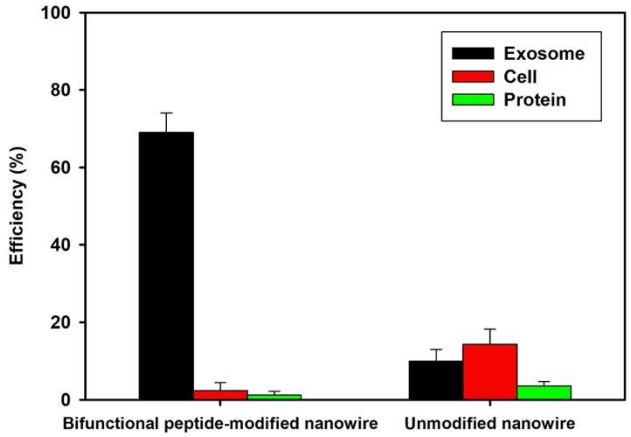

Fig. 6 Evaluation of exosome-collecting efficiency from cell culture medium using bifunctional peptide-modified nanowire platform and unmodified nanowire platform (N=3).

drug delivery. In addition to its exosome-related applications, P238 is likely to be useful in other biological studies, since tetraspanin CD9 is involved in a variety of cellular functions including cell adhesion and migration, cancer cell invasion, egg–sperm fertilization, and virus infection.[48–51]

Linkage of a ZnO binder sequence with P238 (CD9 binder) provides a bifunctional peptide that can directly assemble the ZnO nanowire surface and significantly increase the efficiency of exosome-selective capture and release. With our strategy, it is possible to design bifunctional peptides for additional exosome markers (e.g. CD63, and CD81) and the exosome-targeting efficiency of nanowires may be further improved by co-modification of these peptides.

Notably, the exosome recovery of approximately 70% for this peptide-nanowire platform is comparable to that of an earlier microfluidic device using antibody-modified nanowires.[24] As reported in our previous study,[22] the bare nanowire-anchored microfluidic device with a herringbone pattern could enable extracellular vesicle collection at high efficiency from 1 mL urine with a flow rate of 50 µL/min (20 min collecting time), followed by *in situ* extractions of various miRNAs. We therefore suggest that the increased capture efficiency of nanowires by peptide modification would reduce required sample volumes and shorten collection times relative to the previous unmodified nanowire device under the same processing conditions. Further well-designed microfluidic devices, such as making manifold structures, will enhance the collection efficiency of exosomes because the platform used here has a flat wall and large gap (20 µm) between the nanowire surface and upper channel wall. As demonstrated here, the peptide-nanowire interface allows the captured exosomes to be released without damage, resulting in the utilization of intact exosomes for potential downstream applications such as diagnosis and tailor-made or personalized drug delivery. This peptide interface can be developed in a wide variety of micro-systems, making them an attractive platform for numerous exosome-based applications (e.g., isolation, detection, surface modification, and gene/drug loading). At this point, a startup company (Craif Inc.) has already introduced a ZnO nanowire-based device to the market, and peptides have been widely commercialized. Therefore, commercialization seems quite feasible for this interface. Future studies should focus on further utilizing the peptide-nanowire hybrid interface within practical miniaturized systems for both point-of-care testing and treatment setting. Our findings provide a fundamental strategy to accelerate exosome research.

Conclusion

In the present study, we designed a peptide-nanowire hybrid nanointerface for enhanced capture and release of cancer-derived exosomes within a miniaturized platform. Array-based peptide screening yielded several exosome-binding peptides derived from the sequence of the EWI-2 protein. Among them, P238 (RSHRLRLH) peptide showed relatively high binding to cancer-derived exosomes via CD9 surface protein. P238 was conjugated with a ZnO-binding HCVAHR sequence to obtain a bifunctional peptide for the direct assembly and functionalization of the ZnO surface. Modification by the bifunctional peptide significantly improved the exosome capture efficiency of the ZnO nanowires. The captured exosomes were released from the nanowires by NaCl solution and showed integrity for downstream miRNA analysis. Lastly, our platform showed promise in collecting exosomes from the complicated cell culture medium. We believe that the proposed nanointerface has great potential for application in microfluidic platforms for exosome-based cancer diagnostics and therapeutics.

Experimental section

Binding assay between EWI-2 peptide array and cancer-derived exosomes

The peptide array was prepared by fluorenylmethyloxycarbonyl (Fmoc)-based chemistry using a peptide auto-synthesizer as previously described.[35,36,44] Cancer-derived exosomes were

isolated from the cultured medium of MDA-MB-231 human breast cancer cells by ultracentrifugation. More details are provided in the Supporting Information.

MDA-MB-231-derived exosomes were labeled with CellTracker Orange CMRA (Thermo Fisher Scientific, Waltham, MA, USA) at 3×10^{10} exosome particles/mL and 9 μM fluorescent dye for 30 min.[33] Excess fluorescent dye in the supernatant was removed after ultracentrifugation at 4°C and 110,000 × g for 80 min. The labeled exosome pellet was washed with 0.2-μm-filtered PBS before ultracentrifugation and redispersion with 0.2-μm-filtered PBS. The EWI-2 peptide array was blocked with 5% bovine serum albumin in PBS for 30 min and washed three times with 0.05% Tween 20 in PBS for 3 min. The peptide array was then soaked in a suspension of 1.5×10^{10} fluorescently labeled exosomes/mL for 1 h and washed three times with PBS for 3 min. All steps were performed with a low-speed shaker at room temperature (25°C). Fluorescence scanning and imaging were performed using a biomolecular imager (Typhoon FLA 9500; GE Healthcare, Uppsala, Sweden) using a 550 nm excitation wavelength, 570 nm emission wavelength, and an LPG filter. Spot intensity was quantified using ImageQuant software (GE Healthcare).

SPR measurement

Peptide-binding affinity was studied using the Biacore X100 Plus Package SPR system (GE Healthcare). P238 powder (prepared as shown in the Supporting Information) was dissolved in acetate buffer (pH 5.5) to 500 μg/mL and immobilized on a CM5 sensor chip surface as a ligand using an amine coupling kit (GE Healthcare) with a contact time of 720 s to obtain an immobilized response of approximately 3,000 RU. To determine the K_D for binding of P238 and CD9, CD9 protein (Ab152262; Abcam, Cambridge, UK) was diluted in PBS to 37.5, 75, 150, 300, and 600 nM before sequential injections over the P238-immobilized sensor chip with a contact time of 30 s and dissociation time of 60 s. The K_D was determined using the Biacore X100 evaluation software (GE Healthcare) with a steady-state model. CD9, EpCAM (Ab151338; Abcam), or integrin beta 5 (Ab151845; Abcam) was diluted in PBS to 5 μg/mL and passed over the immobilized chip with a contact time of 30 s and a dissociation time of 60 s to study the selectivity of P238. Prior to the comparison of P238 interaction with MDA-MB-231-derived cancer exosomes (EXOP-105A-1; SystemBio, Palo Alto, CA, USA) and healthy human serum-derived exosomes (EXOP-500A-1; SystemBio), CD9 expression in cancer and healthy exosomes was quantified using the human CD9 ELISA kit (LS-F6853; LifeSpan BioSciences, Seattle, WA, USA). Following the user manual, the diluted exosome suspensions (1 μg total protein) and the prepared standard solutions were applied to the sandwich ELISA assay. Cancer exosomes or healthy exosomes diluted with PBS to 5 μg total protein per mL were injected over the immobilized chip with a contact time of 90 s and dissociation time of 180 s. After each analysis, the immobilized chip was regenerated with 10 mM glycine-HCl pH 2.0 for 60 s. All steps were run with HEPES-buffered saline at 37°C.

Preparation of ZnO nanowire interface within a microfluidic platform

To fabricate the double-channel platform (Fig. S5), a micro-slide glass substrate (S1112; Matsunami Glass Ind., Ltd., Osaka, Japan) was cleaned and positive photoresist (OFPR8600; Tokyo Ohka Kogyo Co. Ltd., Kawasaki, Japan) was spin-coated on it. The substrate was patterned by exposing it to 200 mW/cm^2 ultraviolet light through a photomask; the pattern (1.5 mm in width and 2 cm in length) was developed in an NMD-3 2.38% solution (Tokyo Ohka Kogyo Co. Ltd.). The ZnO seed layer (100 nm) was coated on the substrate using radio frequency sputtering (SVC-700RFII; Sanyu Electron Co. Ltd., Tokyo, Japan). ZnO nanowires were hydrothermally grown on the substrate in a solution containing 20 mM hexamethylenetetramine (HMTA, Wako Pure Chemical Ind. Ltd., Osaka, Japan) and 20 mM zinc nitrate hexahydrate (Thermo Fisher Scientific) at 95°C for 5 h. The photoresist was removed using developer solution 104 (Tokyo Ohka Kogyo Co. Ltd.) and then washed with ultrapure water, dried with nitrogen gas, and stored in a desiccator before use. The ZnO nanowire substrate was observed by FESEM (Supra40vp; Carl Zeiss Meditec AG, Jena, Germany). Microchannel-structured polydimethylsiloxane (PDMS) was prepared by pouring PDMS (Sylgard® 184; Dow Corning Toray Co., Ltd., Tokyo, Japan) on a microchannel mold. The microchannel was 2 mm in width, 2 cm in length, and 20 μm in height. For bonding between the nanowire substrate and the microchannel-structured PDMS, both were treated with plasma (SEDE-PFA; Meiwafosis Co., Ltd., Tokyo, Japan) and then bonded together. Lastly, inlet and outlet tubes (polyether ether ketone tube, 0.26 mm inside diameter, ICT-55P; Institute of Microchemical Technology Co. Ltd., Kanagawa, Japan) were connected to the platform.

Peptide functionalization of ZnO nanowires in a microfluidic platform

For peptide modification, 1 mL of 100 μM bifunctional peptide in PBS was introduced through the platform at a flow rate of 50 μL/min using a syringe pump (KDS-200; KD Scientific Inc., Holliston, MA, USA) before further incubation for 30 min and washing with 1 mL PBS. The excess peptide in both the flowed and washed solutions was quantified using HPLC (LC-20AR; Shimadzu, Kyoto, Japan) to estimate the amount of peptide modified on the nanowire surface. A TSKgel ODS-100Z column (Tosoh Corporation, Shiba, Japan), acetonitrile/water/trifluoroacetic acid (90:10:0.1) mobile phase, and 214-nm absorbance detection were used.

To optimize peptide elution, the ZnO nanowire substrate was modified with the FITC-conjugated bifunctional peptide; then the modified substrate was incubated with 0, 0.125, 0.25, 0.5, 1, 2, or 4 M NaCl solution in 20 mM Tris buffer on a low-speed shaker at 25°C for 30 min. Images of the eluted substrate were taken using a fluorescence microscope (DM6 B; Leica Camera AG, Wetzlar, Germany) and fluorescence intensity was quantified using ImageJ software (NIH, Bethesda, MD, USA).

After peptide modification and elution with 1 M NaCl solution, FESEM was utilized to observe the morphological

changes of the nanowires. The nanowire substrates (2 cm × 4 cm) including modified, eluted, and unmodified substrates (as background) were analyzed using a Fourier transform infrared spectrometer (Nicolet iS50; Thermo Fisher Scientific) with automatic MAIRS equipment (TN10-3000; Thermo Fisher Scientific) to obtain pMAIRS spectra.

Enhanced exosome capture and release of microfluidic nanowire array by bifunctional peptide

For exosome capture, 1 mL MDA-MB-231-derived exosome suspension at 1×10^9 particles/mL was introduced into the microchannel at 50 µL/min using a syringe pump before flowing 20 µL of PBS to remove uncaptured exosomes. The number of exosomes in the flowed and washed solutions was quantified using an NTA instrument (NanoSight LM10; Malvern, Malvern, UK) to calculate the number of captured exosomes. The bifunctional peptide-modified nanowire substrate was observed by FESEM after exosome capture.

For exosome release, 1 mL of 1 M NaCl solution in 20 mM Tris buffer was introduced through the microchannel at 50 µL/min using a syringe pump. The number of exosomes in the flowing NaCl solution was quantified using an NTA instrument to calculate the exosome recovery percentage. FESEM observation of the bifunctional peptide-modified nanowire substrate was also performed after exosome release.

For characterization of the released exosomes, 1 mL of each sample was applied to a measurement cell and analyzed using a Zetasizer (Nano ZS ZEN3600; Malvern) with a protein profile to obtain the zeta potential value. The released exosome suspension was applied to total exosome RNA and protein isolation kit (4478545; Thermo Fisher Scientific) based on phenol-chloroform extraction. Next, the isolated miRNA was quantified using a Qubit microRNA assay kit (Q32880) and Qubit fluorometer (Thermo Fisher Scientific), based on fluorescent reading of miRNA-binding fluorophores. All steps were performed in accordance with the manufacturers' instructions.

Comparison of exosome-collecting efficiency between peptide-nanowire platform and ultracentrifugation

For the peptide-nanowire platform, exosomes were collected as described above. A 1-mL aliquot of MDA-MB-231-derived exosome suspension at 1×10^9 particles/mL was ultracentrifuged at 4°C and 110,000 × g for 80 min. The exosome pellet was redispersed with 0.2-µm-filtered PBS (1 mL). The number of collected exosomes was determined by the NTA system for calculating relative exosome amounts.

Evaluation of the exosome-collecting efficiency from a cultured, cell-suspened medium

MDA-MB-231 cells (HTB-26TM; American Type Culture Collection, Manassas, VA, USA) were cultured in Dulbecco's modified Eagle medium supplemented with 10% exosome-depleted FBS, 1 mM sodium pyruvate, and 100 units/mL of penicillin-streptomycin (Thermo Fisher Scientific). The cultured medium was collected after 48 h of culture at approximately 90% confluency. The cells were then suspended in the collected medium. The prepared sample (1 mL, 1.23×10^7 exosomes/mL, 1.19 µg protein/µL, 4×10^5 cells/mL) was continuously injected into the peptide-modified nanowire platform and the unmodified nanowire platform at a flow rate of 50 µL/min using a syringe pump. PBS (20 µL) was injected to wash the channel before 1 M NaCl solution in 20 mM Tris buffer (1 mL) was injected. Efficiency was calculated by quantifying proteins, exosomes, and in both the prepared eluted samples. The suspended proteins, exosomes, and cells were quantified using a bicinchoninic acid protein assay kit (TaKaRa Bio Inc., Shiga, Japan), exosome ELISA complete Kit (CD9 detection; SystemBio), and cell-counting hemocytometer, respectively. Samples were centrifuged at 2,000 rpm for 10 min to remove the suspended cells before protein and exosome quantification.

Conflicts of interest

There are no conflicts to declare.

Acknowledgements

This work was supported by the Impulsing Paradigm Change through Disruptive Technologies (ImPACT) Program of the Council for Science, Technology, and Innovation (Cabinet Office, Government of Japan) and JSPS KAKENHI grants 18H01795, 18K18970, and 18K04848.

References

1 I. L. Colao, R. Corteling, D. Bracewell and I. Wall, *Mol. Med.,* 2018, **24**, 242–256.
2 G. Van Niel, G. D'Angelo and G. Raposo, *Nat. Rev. Mol. Cell Biol.,* 2018, **19**, 213.
3 T. B. Steinbichler, J. Dudás, H. Riechelmann and I. I. Skvortsova, *Semin. Cancer Biol.*, 2017, **44**, 170–181.
4 S. L. N. Maas, X. O. Breakefield and A. M. Weaver, *Trends Cell Biol.,* 2017, **27**, 172–188.
5 A. Hoshino, B. Costa-Silva, T. Shen, G. Rodrigues, A. Hashimoto, M. T. Mark, H. Molina, S. Kohsaka, A. Di Giannatale, S. Ceder, S. Singh, C. Williams, N. Soplop, K. Uryu, L. Pharmer, T. King., L. Bojmar, A. E. Davies, Y. Ararso, T. Zhang, H. Zhang, J. Hernandez, J. M. Weiss, V. D. Dumont-Cole, K. Kramer, L. H. Wexler, A. Narendran, G. K. Schwartz, J. H. Healey, P. Sandstrom, K. Jørgen Labori, E. H. Kure, P. M. Grandgenett, M. A. Hollingsworth, M. de Sousa, S. Kaur, M. Jain, K. Mallya, S. K. Batra, W. R. Jarnagin, M. S. Brady, O. Fodstad, V. Muller, K. Pantel, A. J. Minn, M. J. Bissell, B. A. Garcia, Y. Kang, V. K. Rajasekhar, C. M. Ghajar, I. Matei, H. Peinado, J. Bromberg and D. Lyden, *Nature,* 2015, **527**, 329–335.
6 P. Reclusa, S. Taverna, M. Pucci, E. Durendez, S. Calabuig, Manca, M. J. Serrano, L. Sober, P. Pauwels, A. Russo and C. Rolfo, *J. Thorac. Dis.,* 2017, **9**, S1373–S1382.
7 S. M. Kim, Y. Yang, S. J. Oh, Y. Hong, M. Seo and M. Jang, *J. Control. Release.,* 2017, **266**, 8–16.
8 T. Yamamoto, N. Kosaka, and T. Ochiya, S*ci. Technol. Adv. Mater.,* 2019, **20**, 746–757.
9 T. Yamashita, Y. Takahashi, and Y. Takakura, *Biol. Pharm. Bull.,* 2018, 41, 835–842.
10 D. D. Taylor and S. Shah, Methods, 2015, **87**, 3–10.
11 P. Li, M. Kaslan, S. H. Lee, J. Yao and Z. Gao, *Theranostics*, 2017, **7**, 789–804.
12 M. Y. Konoshenko, E. A. Lekchnov, A. V. Vlassov, and P. P. Laktionov, *Biomed Res. Int.*, 2018, **2018**, 8545347.

13 M. Zhang, K. Jin, L. Gao, Z. Zhang, F. Li, F. Zhou, L. Zhang, *Small Methods*, 2018, **2**, 1800021.
14 J. C. Contreras-Naranjo, H. J. Wu and V. M. Ugaz, *Lab Chip,* 2017, **17**, 3558–3577.
15 C. L. Hisey, K. D. P. Dorayappan, D. E. Cohn, K. Selvendiran and D. J. Hansford, *Lab Chip*, 2018, **18**, 3144–3153.
16 M. He, J. Crow, M. Roth, Y. Zeng and A. K. Godwin, *Lab Chip,* 2014, **14**, 3773–3780.
17 L. G. Liang, M. Q. Kong, S. Zhou, Y. F. Sheng, P. Wang, T. Yu, F. Inci, W. P. Kuo, L. J. Li, U. Demirci and S. Wang, *Sci. Rep.,* 2017, **7**, 46224.
18 H. K. Woo, V. Sunkara, J. Park, T. H. Kim, J. R. Han, C. J. Kim, H. I. Choi, Y. K. Kim and Y. K. Cho, *ACS Nano*, 2017, **11**, 1360–1370.
19 K. Lee, H. Shao, R. Weissleder and H. Lee, *ACS Nano,* 2015, **9**, 2321–2327.
20 M. Wu, Y. Ouyang, Z. Wang, R. Zhang, P. H. Huang, C. Chen, H. Li, P. Li, D. Quinn, M. Dao, S. Suresh, Y. Sadovsky and T. J. Huang, *Proc. Natl. Acad. Sci. U. S. A.,* 2017, **114**, 10584–10589.
21 Z. Wang, H. Wu, D. Fine, J. Schmulen, Y. Hu, B. Godin, J. X. J. Zhang and X. Liu, *Lab Chip,* 2013, **13**, 2879–2882.
22 T. Yasui, T. Yanagida, S. Ito, Y. Konakade, D. Takeshita, T. Naganawa, K. Nagashima, T. Shimada, N. Kaji, Y. Nakamura, I. A. Thiodorus, Y. He, S. Rahong, M. Kanai, H. Yukawa, T. Ochiya, T. Kawai and Y. Baba, *Sci. Adv.,* 2017, **3**, e1701133.
23 Z. Chen, S. B. Cheng, P. Cao, Q. F. Qiu, Y. Chen, M. Xie, Y. Xu and W. H. Huang, *Biosens. Bioelectron.,* 2018, **122**, 211–216.
24 R. Qi, G. Zhu, Y. Wang, S. Wu, S. Li, D. Zhang, Y. Bu, G. Bhave, R. Han and X. Liu, *Biomed. Microdevices*, 2019, **21(2)**:35.
25 T. Shimada, T. Yasui, A. Yokoyama, T. Goda, M. Hara, T. Yanagida, N. Kaji, M. Kanai, K. Nagashima, Y. Miyahara, T. Kawai, Y. Baba, *Lab Chip,* 2018, **18**, 3225–3229.
26 S. Rahong, T. Yasui, N. Kaji and Y. Baba, *Lab Chip,* 2016, **16**, 1126–1138.
27 S. Rahong, T. Yasui, T. Yanagida, K. Nagashima, M. Kanai, A. Klamchuen, G. Meng, Y. He, F. Zhuge, N. Kaji, T. Kawai and Y. Baba, *Sci. Rep.,* 2014, **4**, 5252.
28 T. Yasui, T. Yanagida, T. Shimada, K. Otsuka, M. Takeuchi, K. Nagashima, S. Rahong, T. Naito, D. Takeshita, A. Yonese, R. Magofuku, Z. Zhu, N. Kaji, M. Kanai, T. Kawai and Y. Baba, *ACS Nano*, 2019, **13**, 2262–2273.
29 H. So, K. Lee, N. Murthy and A. P. Pisano, *ACS Appl. Mater. Interfaces*, 2014, **6**, 20693–20699.
30 C. S. Stipp, T. V. Kolesnikova and M. E. Hemler, *J. Biol. Chem.*, 2001, **276**, 40545–40554.
31 X. A. Zhang, W. S. Lane, S. Charrin, E. Rubinstein and L. Liu, *Cancer Res.,* 2003, **63**, 2665–2674.
32 Y. Yoshioka, Y. Konishi, N. Kosaka, T. Katsuda, T. Kato and T. Ochiya, *J. Extracell. Vesicles*, 2013, **2**, 10.3402/jev.v2i0.20424.
33 E. Hosseini-Beheshti, S. Pham, H. Adomat, N. Li and E. S. Tomlinson Guns, *Mol. Cell. Proteomics,* 2012, **11**, 863–885.
34 R. Frank, *J. Immunol. Methods*, 2002, **267**, 13–26.
35 M. Okochi, M. Muto, K. Yanai, M. Tanaka, T. Onodera, J. Wang, H. Ueda and K. Toko, *ACS Comb. Sci.,* 2017, **19**, 625–632.
36 M. Tanaka, T. Suwatthanarak, A. Arakaki, B. R. G. Johnson, S. D. Evans, M. Okochi, S. S. Staniland and T. Matsunaga, *Biotechnol. J.*, 2018, **13**, 1800087.
37 J. D. Watson and E. J. Milner-White, *J. Mol. Biol.,* 2002, **315**, 171–182.
38 E. J. Milner-White, J. W. M. Nissink and F. H. Allen and W. J. Duddy, *Acta Crystallogr. Sect. D Biol. Crystallogr.,* 2004, **60**, 1935–1942.
39 K. L. Clark, Z. Zeng, A. L. Langford, S. M. Bowen and S. C. Todd, *J. Immunol.* 2001, **167**, 5115–5121.
40 C. Montpellier, B. A. Tews, J. Poitrimole, V. Rocha-Perugini, V. D'Arienzo, J. Potel, X. A. Zhang, E. Rubinstein, J. Dubuisson and L. Cocquerel, *J. Biol. Chem.*, 2011, **286**, 13954–13965.
41 L. G. Trabuco, S. Lise, E. Petsalaki and R. B. Russell, *Nucleic Acids Res.,* 2012, **40**, W423–W427.
42 M. Okochi, T. Sugita, S. Furusawa, M. Umetsu, T. Adschiri and H. Honda, *Biotechnol. Bioeng.,* 2010, **106**, 845–851.
43 A. Care, P. L. Bergquist and A. Sunna, *Trends Biotechnol.*, 2015, **33**, 259–268.
44 M. Tanaka, I. H. Harlisa, Y. Takahashi, N. A. Ikhsan and M. Okochi, *RSC Adv.*, 2018, **8**, 8795–8799.
45 J. Li, C. Qi, Z. Lian, Q. Han, X. Wang, S. Cai, R. Yang, C. Wang, *ACS Appl. Mater. Interfaces*, 2016, **8**, 2511–2516.
46 M. Salehi and M. Sharifi, *J. Cell. Physiol.,* 2018, **233**, 6370–6380.
47 C. Bing, X. Zijing, D. Ya-Nan, Y. Yanfang, Z. Peng, Z. Hongxia, X. Ningzhi and L. Shufang, *Open Biol.,* 2019, **9**, 180212.
48 G. Rappa, T. M. Green, J. Karbanová, D. Corbeil and A. Lorico,. *Oncotarget*, 2015, **6**, 7970–7991.
49 Y. Miki, M. Yashiro, T. Okuno, K. Kitayama, G. Masuda, K. Hirakawa and M. Ohira, *Br. J. Cancer,* 2018, **118**, 867–877.
50 K. Yoshida, N. Kawano, Y. Harada and K. Miyado, in *Sexual Reproduction in Animals and Plants*, ed. H. Sawada, N. Inoue, M. Iwano, Springer, Tokyo, 2014, ch. 31, 383–391.
51 R. Umeda, Y. Satouh, M. Takemoto, Y. Nakada-Nakura, K. Liu, T. Yokoyama, M. Shirouzu, S. Iwata, N. Nomura, K. Sato, M. Ikawa, T. Nishizawa, and O. Nureki, *Nat. Commun.,* 2020, **11**, 1606.

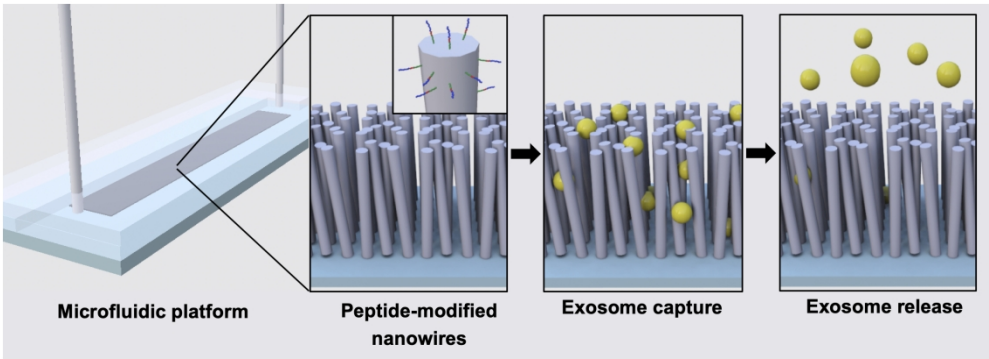

460x169mm (144 x 144 DPI)